Finite Elements in Analysis and Design 47 (2011) 796–803

Contents lists available at ScienceDirect

Finite Elements in Analysis and Design

journal homepage: www.elsevier.com/locate/finel

Development of super-convergent plane stress element formulation using an inverse approach

H. Ahmadian [a,*], S. Farughi [b]

[a] Center of Excellence in Experimental Solid Mechanics and Dynamics, School of Mechanical Engineering, Iran University of Science and Technology, Narmak, Tehran 16844, Iran
[b] School of Mechanical Engineering, Urmia University of Technology, Band Street, Urmia, Iran

ARTICLE INFO

Article history:
Received 30 October 2009
Received in revised form
2 February 2011
Accepted 25 February 2011
Available online 21 March 2011

Keywords:
Plane stress element
Inverse method
Discretization error

ABSTRACT

New formulation for the plane stress element with super-convergent properties is presented using an inverse method. The element formulation is developed in parametric form satisfying geometrical symmetries of the element and producing rigid body and constant strain modes requirements. The remaining higher order modes of the element are assigned by minimizing the difference between the resultant parametric finite element discrete formulation and the corresponding continuous governing equations, i.e. the discretization errors. Classically minimization of discretization errors is performed by starting from the lowest order error terms and setting them equal to zero. In this paper, it is shown the effect of these errors may also be minimized by allowing the residual errors in adjacent nodes to be equal in magnitudes but with opposite signs. This causes zero bias error in the associated eigen-problem and leads to an element model with super convergent eigen-solution properties. The proposed method of minimizing the errors is applied to the plane stress element formulation and it is proven a more accurate model is achieved over the classical method of error minimization. The new element formulation result super-convergent eigen-solution and in a numerical example these convergence properties are compared to the reported models in the literature.

1. Introduction

In-plane stress elements considered in this paper are a class of elements with translational degrees of freedom at nodes representing in-plane displacements. In the earlier studies, plane stress elements were developed using linear displacement assumption (LDS). The rectangular element model developed by Argyris and Kelsey [2] using bilinear shape functions belong to this group of elements. Later, linear stress assumption approach (LSA) was introduced by Przemieniecki and Berke [3] who employed this concept in driving a new element formulation. However, these formulations result stiff elements for problems in which the response is dominated by linear strain gradients. In these models, over-stiffness increases rapidly as aspect ratio of the element increases [4].

There are various proposals to improve the bending behavior of the standard bilinear rectangle elements among them are classic Pain's hybrid formulation [5] and nonconforming formulations of Wilson et al. [6] and Taylor et al. [7]. However, the formulations presented in [3,5,6] lead to the same stiffness matrix for the nodal displacements when the mesh is rectangular and aligned with the global Cartesian co-ordinates [8,9]. More recently, Felippa [10] showed the best model for rectangular plane stress is assumed linear stress formulation. This is also reported by Yunhua and Eriksson [11] for rectangular in-plane element.

In the current paper, an inverse approach is employed to obtain the optimum element formulation which leads to results with super-convergent properties. The advantage of employing the inverse method is providing the best possible formulation for the element under consideration. Whereas using classical finite element method, the obtained results are dependent to the selection of the element shape functions and the best element formulation may not always be achieved. Inverse approach in finite element formulation was used by Argyris et al. [12], Bergan and Nygard [13], and Simo and Rifai [14] to enforce constraints, in the form of assumed strain modes, on the stiffness formulation to guarantee that the element model would pass the patch test. Stavrinidis et al. [15] introduced discretization error of rod and beam elements by power series ofΔx, where Δx is the element characteristic of length. Discretization errors are those associated with replacing the continuous media by one composed of finite elements. If the elements characteristic of length approaches to zero, the discretization errors vanishes. Stavrinidis et al. [15] obtained new formulations for beam and rod element by minimizing the discretization errors. Later, Ahmadian et al. [16] developed mass and stiffness matrices of a rectangular plate element by minimizing the finite element model discretization errors.

* Corresponding author. Tel.: +98 21 77240198; fax: +98 21 77240488.
E-mail address: ahmadian@iust.ac.ir (H. Ahmadian).

0168-874X/$ - see front matter © 2011 Elsevier B.V. All rights reserved.
doi:10.1016/j.finel.2011.02.010

The objective in this paper is to set up admissible parametric stiffness and mass matrices for rectangular plane stress element. A parametric model for the element is developed and the unknown parameters are defined by using a different approach in minimizing the discretization errors. The present paper proposes two significant improvements to the inverse finite element model development. The first improvement is achieved by employing the constant strain modes to introduce more constraint on the stiffness matrix parameters and reduce the number of generic element unknowns. The second contribution of the present paper is the strategy used in minimizing the discretization errors. Previous proposals in inverse finite element modeling [15,16] start from the lowest order terms and set the discretization errors to zero. However there are situations as will be shown later in this paper where using the available parameters the error terms cannot be set to zero. This paper distributes the errors in these situations evenly over the entire domain with opposite sings in neighboring nodes. This does not affect the accuracy of the eigen-value and displacement predictions and allows more accurate models to be identified. The obtained stiffness and mass model produces highly accurate eigen-solution and displacement having fast rate of convergence. These improvements are assessed analytically and also through comparing the convergence rates of the obtained optimal model with those of existing models.

The paper is outlined as follows. In section two, the physical requirements of an element model is discussed. These physical requirements are then used to develop a parametric model for the element. Section 3 demonstrates the procedure of parameterization and identification of optimum parameters using a simple four node membrane element. Section 4 uses the inverse strategy introduced in Section 3 in order to establish a new formulation for the rectangular plane stress element. Section 5 investigates the convergence rates of the obtained stiffness and mass formulations using numerical examples. Some concluding remarks are made in Section 6.

2. Physical requirements of an element model

In general, an element model must meet certain requirements. Consider an element with d degrees of freedom and R rigid-body modes. The stiffness matrix $\boldsymbol{K}$ is symmetric positive semi-definite and of rank $d-r$ and the rigid-body modes of the element, $\Phi_R=[\phi_{R1},\phi_{R2},...,\phi_{Rr}]$ form its null space:

$$K\Phi_R=0 \tag{1}$$

Also mass matrix M is symmetric positive-definite and of rank d. If the rigid-body modes are defined on the principal coordinates of the element then,

$$\Phi_R^T M\Phi_R=diag(m,m,m,I_{xx},I_{yy},I_{zz}) \tag{2}$$

where m is the element mass and I_{xx}, I_{yy}, and I_{zz} are the moments of inertia. Moreover, if some strain modes of the element such as constant strain modes, $\Phi_C=[\phi_{c1},\phi_{c2},...,\phi_{cn}]$, are known then further constraints can be imposed on the stiffness matrix:

$$K\phi_{ci}=\lambda_i\phi_{ci},\quad i=1,2,\ldots,n \tag{3}$$

where λ_i corresponds to the strain energy stored in the element volume V at the ith strain mode. The strain energy in each mode is defined using the known strain, ε_i, and stress, σ_i, distributions over the element domain as,

$$\lambda_i=\frac{1}{2}\int_V \varepsilon_i\sigma_i\,dv \tag{4a}$$

The orthogonality relations for the set of rigid body modes and constant strain modes are

$$\begin{bmatrix}\Phi_R & \Phi_C\end{bmatrix}^T K\begin{bmatrix}\Phi_R & \Phi_C\end{bmatrix}=\begin{bmatrix}0 & 0\\ 0 & \Gamma\end{bmatrix},\quad \Gamma=diag(\lambda_1,\lambda_2,\ldots,\lambda_n) \tag{4b}$$

The element will pass its associated patch test if it has the ability to model the rigid body motion and constant strain mode [9]. Therefore when Φ_C contains all the element constant strains modes, the element formulation satisfies the patch test requirements necessary for solution convergence. Further requirements regarding the entries of stiffness and mass matrices can be defined using geometrical symmetries of the element. If the element has some symmetrical properties, then the mass and stiffness models reflect these properties; rotation of the element about its symmetry axes does not change the stiffness and mass matrices. It is possible to define a family of stiffness and mass matrices for an element that satisfies these requirements but depend upon one or more parameters.

In the following section, a simple example is provided to demonstrate the procedure of inverse model development. The example involves generating stiffness model of a transverse membrane element. A parametric stiffness model is developed by imposing the physical requirements on the stiffness model. Admissible parametric form of stiffness matrices has one unattributed parameter that is assigned by minimizing the discretization errors.

3. Four-nodes rectangular transverse membrane element

Membrane elements are a class of elements used for modeling thin structures that are subjected to tension. They have only out-of-plane degrees of freedom, possess negligible resistance to bending moments, and restoring forces arise exclusively from in-plane stretching or tensile forces [17]. These elements are used widely in analysis of acoustic fields. The transverse membrane element reported in the literature is developed based on linear displacement assumption [1]. The resultant stiffness matrix presents a second order convergence rate for static deflection problems.

A four-node rectangular membrane element with dimensions of Δx and Δy, shown in Fig. 1, is considered. Each node has one degree of freedom and the element stiffness matrix is a 4×4 symmetric positive semi-definite matrix of the following general form:

$$K=\kappa\begin{bmatrix}k_{11} & k_{12} & k_{13} & k_{14}\\ & k_{22} & k_{23} & k_{24}\\ & & k_{33} & k_{34}\\ sym & & & k_{44}\end{bmatrix} \tag{5}$$

where κ is a positive real scalar. The element has two symmetry axes; when the element is rotated through π radians about one of these axes the stiffness matrix remains unchanged. The rotations are equivalent to applying the transformations T_{xx} and T_{yy} as

$$T_{xx}^T KT_{xx}=K,\quad T_{yy}^T KT_{yy}=K,\quad T_{xx}=\begin{bmatrix}0 & -1 & 0 & 0\\ -1 & 0 & 0 & 0\\ 0 & 0 & 0 & -1\\ 0 & 0 & -1 & 0\end{bmatrix},$$

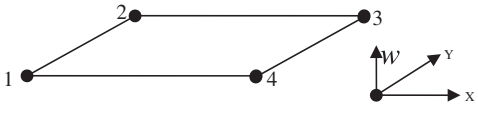

Fig. 1. Four-node square membrane element.

$$T_{yy}=\begin{bmatrix}0&0&0&-1\\0&0&-1&0\\0&-1&0&0\\-1&0&0&0\end{bmatrix} \tag{6}$$

Using the physical symmetry requirements, the number of unknown parameters of stiffness matrix reduces to 4:

$$K=\kappa\begin{bmatrix}k_{11}&k_{12}&k_{13}&k_{14}\\&k_{11}&k_{14}&k_{13}\\&&k_{11}&k_{12}\\sym&&&k_{11}\end{bmatrix} \tag{7}$$

When the element is rotated through $\pi/2$ radians in its own plane, the element aspect ratio $q=\Delta y/\Delta x$, is reversed. This rotation is equivalent to the transformation of,

$$T_{zz}=\begin{bmatrix}0&0&0&1\\1&0&0&0\\0&1&0&0\\0&0&1&0\end{bmatrix},\quad T_{zz}^{T}K(q)T_{zz}=K(1/q) \tag{8}$$

It leads directly from Eq. (8) that k_{14} is obtained by inverting the aspect ratio q *to* $1/q$ ink_{12}; this produces one more constraint on the parameters of the element.

The element has one rigid-body mode,

$$\Phi_r=\begin{bmatrix}1&1&1&1\end{bmatrix}^T \tag{9}$$

Introducing the above rigid body mode into Eq. (1), one more parameter is defined as,

$$K\Phi_r=0\Rightarrow k_{13}=-(k_{11}+k_{12}+k_{14}) \tag{10}$$

This brings the total number of unattributed parameters of the parametric stiffness matrix to three. The element has two constant strain modes,

$$\phi_{C1}=\begin{bmatrix}-\frac{1}{2}&\frac{1}{2}&\frac{1}{2}&-\frac{1}{2}\end{bmatrix}^T,\quad \phi_{C2}=\begin{bmatrix}-\frac{1}{2}&-\frac{1}{2}&\frac{1}{2}&\frac{1}{2}\end{bmatrix}^T \tag{11}$$

The constant strain modes ϕ_{Ci}, $i=1,2$ produce the following stored strain energy in the entire element:

$$\lambda_1=\frac{P}{q},\quad \lambda_2=Pq \tag{12}$$

where P is the surface tension of the element. Employing the relation defined in Eq. (3) one finds the following relations:

$$k_{12}=\frac{Pq}{2\kappa}-k_{11},\quad k_{14}=\frac{P}{2q\kappa}-k_{11} \tag{13}$$

Now the unknown parameters of stiffness matrix are reduced to one. The unknown parameter is determined by minimizing the discretization errors of the element formulations. The finite element formulation obtained from the parametric stiffness matrix is compared with the governing equation of transverse membrane allowing identification of the unattributed parameter by minimizing the discretization errors.

The membrane elements with area $\Delta A=\Delta x\Delta y$ are assembled to create a regular mesh for a four-node rectangular membrane element with free edges as shown in Fig. 2. In the assembled model, one discrete equations of motion for a typical internal node (i, j) is formed. This discrete governing equation is then converted to continuous series form by defining the deformations in the neighboring nodes using Taylor series expansions of deformations in node (i, j),

$$d_{i\pm1,j\pm1}=d_{i,j}+\sum_{n=1}^{\infty}\frac{1}{n!}\left(\pm\Delta x\frac{\partial}{\partial x}\pm\Delta y\frac{\partial}{\partial y}\right)^n d_{i,j} \tag{14}$$

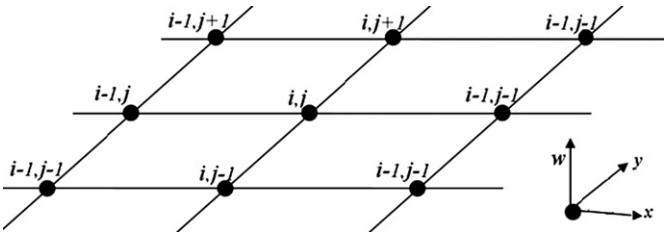

Fig. 2. Assembled square membrane elements.

This process transforms the discrete finite element equations into a partial differential equation having terms of increasing order of smallness $O(\Delta x^{2n},\Delta y^{2n})$ $n=1, 2,\ldots$. The resultant continuous differential equations must produce the governing equation of motion and boundary conditions for transverse membrane motion [17]:

$$P\left(\frac{\partial^2 w}{\partial x^2}+\frac{\partial^2 w}{\partial y^2}\right)+F(x,y)=0$$
$$\left.\frac{\partial w}{\partial x}\right|_{x=0,\Delta x}=0,\quad \left.\frac{\partial w}{\partial y}\right|_{y=0,\Delta y}=0 \tag{15}$$

where P is the surface tension of element and $F(x,y)$ is the external lateral force.

The differential equations in internal nodes of the assembled model are of even orders of Δx and differential equations corresponding to the boundary and corner nodes contain all orders of Δx. First, the second-order terms in the internal nodes are compared with the classical membrane Eq. (15), and if the differential equation is satisfied at that order of smallness, the fourth-order terms are investigated, and so on, until the unattributed stiffness parameters are exhausted.

The internal nodes second-order terms form the following partial deferential equation:

$$P\left[\frac{\partial^2 w}{\partial x^2}+\frac{\partial^2 w}{\partial y^2}\right]=0 \tag{16}$$

Eq. (16) represents the equation of motion of membrane theory. Next, the fourth order term of internal nodes is considered:

$$\Delta A^2 P\left[\frac{\partial^2}{\partial x^2}\left(\frac{1}{12q}\frac{\partial^2 w}{\partial x^2}+\left(\frac{1}{4q}+\frac{q}{4}-\frac{\kappa k_{11}}{2}\right)\frac{\partial^2 w}{\partial y^2}\right)\right.$$
$$\left.+\frac{\partial^2}{\partial y^2}\left(\frac{q}{12}\frac{\partial^2 w}{\partial y^2}+\left(\frac{1}{4q}+\frac{q}{4}-\frac{\kappa k_{11}}{2}\right)\frac{\partial^2 w}{\partial x^2}\right)\right]=0 \tag{17}$$

Eq. (17) represents the equation of motion (15) if $\kappa=P$and the following requirements are met:

$$\frac{1}{4}\left(\frac{1}{q}+q-2k_{11}\right)=\frac{q}{12} \tag{18}$$

$$\frac{1}{4}\left(\frac{1}{q}+q-2k_{11}\right)=\frac{1}{12q} \tag{19}$$

Obviously the two Eqs. (18)–(19), cannot be satisfied for different aspect ratios q, therefore one may look for a least squares solution by assigning

$$k_{11}=\frac{5}{12}\left(q+\frac{1}{q}\right) \tag{20}$$

The residues of Eq. (17) would be zero if and only if the aspect ratio q is unity and the discretization errors are of sixth order. One may evaluate the discretization errors in the boundary nodes using the expression defined in Eq. (20). This would lead to fourth order discretization errors in the boundary nodes.

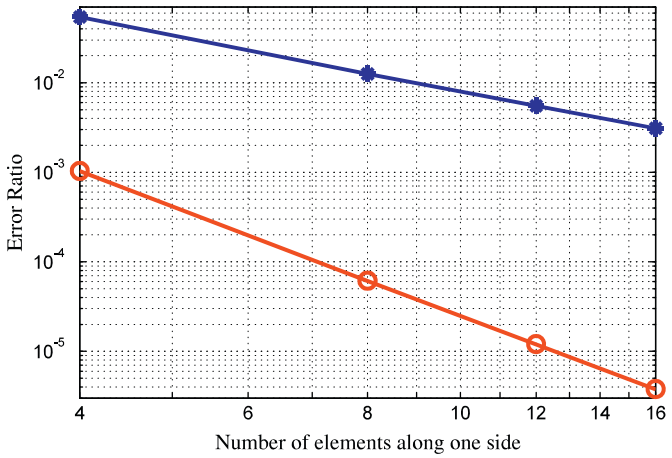

Fig. 3. Errors in estimating mid node deflection of a square membrane (circles – proposed model, stars – bi-linear shape function).

The performance of the newly developed model and its convergence properties are demonstrated using a numerical example. A clamped square membrane with area of A, surface tension of P, subjected to uniformly distributed load F, is modeled using two different formulations namely the stiffness model obtained from bi-linear shape functions and the stiffness matrix developed using inverse approach. The center deflection δ of the membrane obtained from exact solution is $\delta = 0.1474(FA/P)$. Fig. 3 shows the error in estimation of the static deflection of membrane center node as the number of elements is uniformly increased. As shown in Fig. 3, the convergence rate in the bi-linear model is of second order while the convergence rate of the model formed using the proposed stiffness matrix is of fourth order. This example demonstrates the parameterization and error analysis steps required in developing finite element models using an inverse approach.

In the following, a parametric model for rectangular plane stress element is established and the element parameters are obtained using an inverse approach. The error minimization is performed by a new approach which distributes the errors uniformly over the entire domain and sets the cumulative errors to zero.

4. Parametric plane stress model

A rectangular plane stress element with four nodes, two degrees of freedoms per node is considered. The displacement vector of element is

$$d = [d_1, d_2, d_3, d_4]^T, \quad d_i = [u_i, v_i], \quad i = 1,\ldots,4 \tag{21}$$

where u_i and v_i correspond to the displacements at node i in direction of X and Y as shown in Fig. 4. Also the element dimensions are Δx *and* Δy. The element has 8×8 symmetric positive-definite mass matrix and positive semi-definite stiffness matrix as,

$$K = \kappa \begin{bmatrix} K_{11} & K_{12} & K_{13} & K_{14} \\ & K_{22} & K_{23} & K_{24} \\ & & K_{33} & K_{34} \\ sym & & & K_{44} \end{bmatrix}, M = \Delta x \Delta y \begin{bmatrix} M_{11} & M_{12} & M_{13} & M_{14} \\ & M_{22} & M_{23} & M_{24} \\ & & M_{33} & M_{34} \\ sym & & & M_{44} \end{bmatrix} \tag{22}$$

In Eq. (22) κ is a positive real scalar, and $K_{ij}, M_{ij}, \quad i,j = 1,\ldots,4$ are 2×2 sub-matrices. In general, the stiffness and mass matrices of plane stress element have 36 unknown parameters. The element has two symmetric axes as shown in Fig. 4. Rotation of the element by π radians about one of these axes does not affect the stiffness and mass models. These rotations are equivalent to transforming the mass and stiffness matrices using the following transformation matrices:

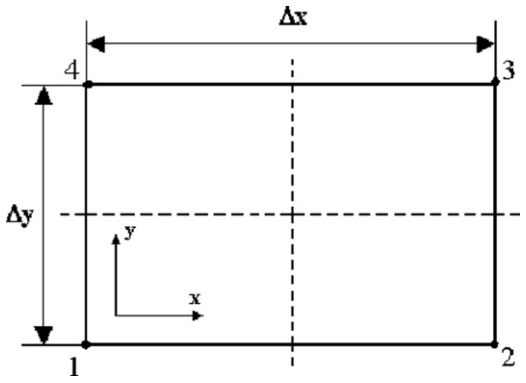

Fig. 4. Rectangular plane stress element.

$$T_{xx} = \begin{bmatrix} 0 & 0 & 0 & R \\ 0 & 0 & R & 0 \\ 0 & R & 0 & 0 \\ R & 0 & 0 & 0 \end{bmatrix}, \quad T_{yy} = \begin{bmatrix} 0 & S & 0 & 0 \\ S & 0 & 0 & 0 \\ 0 & 0 & 0 & S \\ 0 & 0 & S & 0 \end{bmatrix} \tag{23}$$

where

$$R = \begin{bmatrix} 1 & 0 \\ 0 & -1 \end{bmatrix}, \quad S = \begin{bmatrix} -1 & 0 \\ 0 & 1 \end{bmatrix} \tag{24}$$

Applying these transformations, one obtains

$$T_{yy}^T K T_{yy} = K, \quad T_{xx}^T K T_{xx} = K$$
$$T_{yy}^T M T_{yy} = M, \quad T_{xx}^T M T_{xx} = M \tag{25}$$

Applying the constraints introduced in (25) the number of independent parameters in the stiffness and mass matrices is reduced from 36 to 12.

The plane stress element has the three rigid body modes,

$$\Phi_R^T = \begin{bmatrix} 1 & 0 & 1 & 0 & 1 & 0 & 1 & 0 \\ 0 & 1 & 0 & 1 & 0 & 1 & 0 & 1 \\ -q/2 & 1/2 & -q/2 & -1/2 & q/2 & -1/2 & q/2 & 1/2 \end{bmatrix}$$
$$q = \Delta y/\Delta x \tag{26}$$

The rigid-body modes occupy the null space of K, as expressed in Eq. (1). This leads to six independent equations and the number of independent parameters in the stiffness matrix reduces to 6. The plane stress element also has three constant modes as,

$$\Phi_C^T = \begin{bmatrix} -1/2 & 0 & -1/2 & 0 & 1/2 & 0 & 1/2 & 0 \\ 0 & -1/2 & 0 & 1/2 & 0 & 1/2 & 0 & -1/2 \\ -q/2 & -1/2 & q/2 & -1/2 & q/2 & 1/2 & -q/2 & 1/2 \end{bmatrix}$$
$$q = \Delta y/\Delta x \tag{27}$$

Introducing these constant strain modes into Eq. (3) and using Eq. (4), three more parameters are defined,

$$k_{14} = \frac{Eh(1-4k_{12}(1+\upsilon))}{4\kappa(1+\upsilon)}, \quad k_{13} = \frac{Eh(2k_{11}(\upsilon^2-1)+q)}{2\kappa(1-\upsilon^2)}$$
$$k_{28} = \frac{Eh(2qk_{22}(\upsilon^2-1)+1)}{2\kappa q(1-\upsilon^2)} \tag{28}$$

The number of independent parameters in stiffness matrix reduces to 3; these independent parameters are selected as k_{11}, k_{12}, k_{22}. The parametric stiffness of plane stress element can

be defined using these three independent parameters as

$$K_{11}=K_{33}=\begin{bmatrix}k_{11} & k_{12}\\ k_{12} & k_{22}\end{bmatrix},\quad K_{22}=K_{44}=S^TK_{11}S,\quad K_{24}=S^TK_{13}S$$
$$K_{12}=K_{34}=\begin{bmatrix}k_{13} & k_{14}\\ -k_{14} & -k_{22}+q(k_{12}+k_{14})\end{bmatrix},$$
$$K_{14}=K_{23}^T=\begin{bmatrix}k_{11}-\frac{1}{q}(k_{12}+k_{14}) & -k_{14}\\ k_{14} & k_{28}\end{bmatrix}$$
$$K_{13}=\begin{bmatrix}\frac{1}{q}(k_{12}+k_{14})-k_{13} & -k_{12}\\ -k_{12} & -q(k_{12}+k_{14})-k_{28}\end{bmatrix} \tag{29}$$

Appling rigid body modes (26) and using Eq. (2), the unknown parameters in mass matrix of plane stress reduce to 9,

$$M_{11}=M_{33}=\begin{bmatrix}m_{11} & m_{12}\\ m_{12} & m_{22}\end{bmatrix},\quad M_{12}=M_{34}=\begin{bmatrix}m_{13} & m_{14}\\ -m_{14} & -m_{24}\end{bmatrix},$$
$$M_{22}=M_{44}=R^TM_{11}R$$
$$M_{13}=\begin{bmatrix}m_{15} & m_{16}\\ m_{16} & m_{26}\end{bmatrix},\quad M_{23}=R^TM_{14}R,\quad M_{24}=R^TM_{13}R$$
$$M_{14}=\begin{bmatrix}-m_{11}-m_{13}-m_{15}+\frac{1}{4} & m_{13}+m_{15}+m_{12}+m_{14}-m_{16}+m_{22}-m_{24}+\frac{1}{12}\\ m_{24}-m_{15}-m_{12}-m_{14}+m_{16}+m_{22}-m_{13}-\frac{1}{12} & -m_{22}-m_{24}-m_{26}+\frac{1}{4}\end{bmatrix} \tag{30}$$

These unknown parameters are determined by converting the discrete finite element equations to continuous partial differential equations and comparing them with the in-plane displacement governing equations.

In order to perform the error analysis, the elements with equal areas of $\Delta A=\Delta x\Delta y$ are assembled to create a regular mesh for a rectangular membrane with free edges. Fig. 5 shows four elements connected at a common node (i, j). Using the Taylor series expansion the finite element discrete equations in each node can be converted to continuous partial differential equations having terms of increasing order of smallness, $O(\Delta x^{2n}, \Delta y^{2n})$, $n=1, 2, \ldots$. These partial differential equations are compared with the in-plane displacement governing equations in horizontal and vertical directions [18]:

$$\mathrm{Eh}\left(\frac{1}{1-\upsilon^2}\frac{\partial^2u}{\partial x^2}+\frac{1}{2(1-\upsilon)}\frac{\partial^2v}{\partial x\partial y}+\frac{1}{2(1+\upsilon)}\frac{\partial^2u}{\partial y^2}\right)=\rho\frac{\partial^2u}{\partial t^2} \tag{31}$$

$$\mathrm{Eh}\left(\frac{1}{2(1+\upsilon)}\frac{\partial^2v}{\partial x^2}+\frac{1}{2(1-\upsilon)}\frac{\partial^2u}{\partial x\partial y}+\frac{1}{1-\upsilon^2}\frac{\partial^2v}{\partial y^2}\right)=\rho\frac{\partial^2v}{\partial t^2} \tag{32}$$

The comparison of continuous differential equations in series form with the exact governing equations is started from the lowest order terms. The zero and first order terms of internal and boundary nodes introduce no new information on unknown parameters. The second order terms of internal nodes in the X and Y directions are

$$\kappa\left(\frac{1}{1-\upsilon^2}\frac{\partial^2u}{\partial x^2}+4k_{12}\frac{\partial^2v}{\partial x\partial y}+\frac{1}{2(1+\upsilon)}\frac{\partial^2u}{\partial y^2}\right)=\rho\frac{\partial^2u}{\partial t^2} \tag{33}$$

$$\kappa\left(\frac{1}{1-\upsilon^2}\frac{\partial^2u}{\partial x^2}+4k_{12}\frac{\partial^2v}{\partial x\partial y}+\frac{1}{2(1+\upsilon)}\frac{\partial^2u}{\partial y^2}\right)=\rho\frac{\partial^2v}{\partial t^2} \tag{34}$$

Comparing Eqs. (33)–(34) with governing Eqs. (31)–(32), one obtains,

$$k_{12}=\frac{1}{8(1-\upsilon)};\quad \kappa=Eh \tag{35}$$

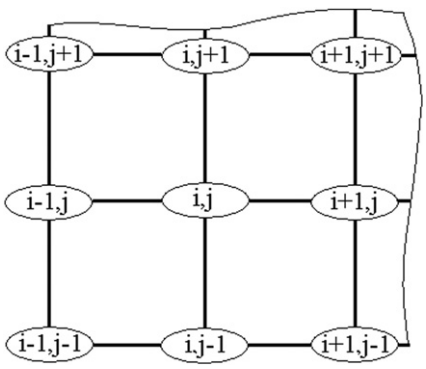

Fig. 5. Assembled plane stress model.

First order terms in boundary nodes lead to the boundary condition requirements,

$$\frac{q}{\upsilon^2-1}\left(\frac{\partial u}{\partial x}+\upsilon\frac{\partial v}{\partial y}\right) \tag{36}$$

$$\frac{q}{2(1+\upsilon)}\left(\frac{\partial u}{\partial y}+\frac{\partial v}{\partial x}\right) \tag{37}$$

The number of parameters in the stiffness matrix (29) is reduced to 2 unknowns of k_{11} and k_{22}. Further constrains are imposed on the entries of the rectangular plane stress stiffness matrix by considering rotation of the element about an axis normal to its plane. The element has an aspect ratio of $q=\Delta y/\Delta x$ and rotation of the element about normal axis to its plane by $\pi/2$ radians changes q to $1/q$ in the stiffness and mass entries,

$$K\left(\frac{1}{q}\right)=T_{zz}^TK(q)T_{zz},\quad T_{zz}=\begin{bmatrix}0 & 0 & 0 & Q\\ Q & 0 & 0 & 0\\ 0 & Q & 0 & 0\\ 0 & 0 & Q & \end{bmatrix},\quad Q=diag(1,-1)$$
$$M\left(\frac{1}{q}\right)=T_{zz}^TM(q)T_{zz} \tag{38}$$

Using this constraint, one concludes k_{11} is converted to when q is changed to $1/q$ and therefore they may be rewritten in the following form:

$$k_{11}=\frac{\alpha}{q}+\beta q,\quad k_{22}=\alpha q+\frac{\beta}{q} \tag{39}$$

Also using constraint (38) the numbers of independent parameters in mass matrix is reduced to 5; these are selected as m_{11}, m_{12}, m_{14}, m_{15}, and m_{16}.

So far the second order error terms in the internal nodes and the first order terms on the boundaries are set to zero. To determine k_{11}, k_{22}, and also the unknown parameters of mass matrix the fourth order errors of internal nodes, the third order error terms on the boundary edges and second order error terms on the corner nodes are investigated simultaneously. This is due

to the fact that accumulated errors of each set of nodes, mid, boundary and corner nodes are of the same order. Only the equations associated with the X direction are considered as these equations are the same as those associated with the Y direction when the aspect ratio is changed from q to $1/q$. The fourth-order terms at internal nodes are,

$$\begin{aligned}&\frac{Eh}{24q(1-\upsilon^2)}\frac{\partial^2}{\partial x^2}\left(2\frac{\partial^2 u}{\partial x^2}+2(1+\upsilon)\frac{\partial^2 v}{\partial x\partial y}+(24\alpha(\upsilon^2-1)+6(1-\upsilon))\frac{\partial^2 u}{\partial y^2}\right)\\&+\frac{Ehq}{24(1-\upsilon^2)}\frac{\partial^2}{\partial y^2}\left((24\beta(\upsilon^2-1)+12)\frac{\partial^2 u}{\partial x^2}+2(1+\upsilon)\frac{\partial^2 v}{\partial x\partial y}+(1-\upsilon)\frac{\partial^2 u}{\partial y^2}\right)\\&-\frac{1}{q}\left(2m_{15}+2m_{14}+\frac{1}{3}+m_{12}-m_{16}-2m_{11}\right)\frac{\partial^2 u}{\partial x^2\partial t^2}\\&+\left(\frac{1}{6}-2m_{14}-m_{12}\right)\frac{q\partial^2 u}{\partial y^2\partial t^2}+4m_{16}\frac{\partial^2 v}{\partial y\partial x\partial t^2}=0\end{aligned}\tag{40}$$

while the third-order terms at boundary edges are,

$$\begin{aligned}&\frac{Eh}{24q(1-\upsilon^2)}\frac{\partial}{\partial x}\left(4\frac{\partial^2 u}{\partial x^2}+4(1+\upsilon)\frac{\partial^2 v}{\partial x\partial y}+(24\alpha(\upsilon^2-1)+6(1-\upsilon))\frac{\partial^2 u}{\partial y^2}\right)\\&+\frac{Ehq}{24(1-\upsilon^2)}\frac{\partial}{\partial y^2}\left((24\beta(\upsilon^2-1)+12)\frac{\partial u}{\partial x}+4\upsilon\frac{\partial v}{\partial y}\right)\\&-q\left(m_{12}+\frac{1}{72}\right)\frac{\partial^2 v}{\partial y\partial t^2}\\&-\frac{1}{q}\left(2m_{15}+2m_{14}+\frac{1}{3}+m_{12}-m_{16}-2m_{11}\right)\frac{\partial^2 u}{\partial x\partial t^2}=0\end{aligned}\tag{41}$$

and the second-order terms at four corner nodes are

$$\begin{aligned}&\frac{Eh}{8q(1-\upsilon^2)}\frac{\partial}{\partial x}\left((1-\upsilon)\frac{\partial v}{\partial x}+(8\alpha(\upsilon^2-1)+2(1-\upsilon))\frac{\partial u}{\partial y}\right)\\&+\frac{Eh}{8(1-\upsilon^2)}\left(2\frac{\partial^2 u}{\partial x^2}+(1+\upsilon)\frac{\partial^2 v}{\partial x\partial y}+(1-\upsilon)\frac{\partial^2 u}{\partial y^2}\right)-\frac{1}{4}\frac{\partial^2 u}{\partial t^2}\\&\times\frac{Ehq}{8(1-\upsilon^2)}\frac{\partial}{\partial y}\left((8\beta(\upsilon^2-1)+4)\frac{\partial u}{\partial x}+2\upsilon\frac{\partial v}{\partial y}\right)-(m_{12}+m_{16})\frac{\partial^2 v}{\partial t^2}\end{aligned}\tag{42}$$

The above equations have terms with coefficients of q, and as the aspect ratio of the element is an arbitrary parameter each of these terms must represent the in-plane governing equation of motions or associated boundary conditions independently. The stiffness terms of Eqs. (40) and (41) with coefficient q^{-1} are

$$\begin{aligned}&\frac{Eh}{q}\frac{\partial^2}{\partial x^2}\left(\frac{1}{12(1-\upsilon^2)}\frac{\partial^2 u}{\partial x^2}+\frac{1}{12(1-\upsilon)}\frac{\partial^2 v}{\partial x\partial y}+\frac{\Delta}{(1+\upsilon)}\frac{\partial^2 u}{\partial y^2}\right)\\&\frac{Eh}{q}\frac{\partial}{\partial x}\left(\frac{1}{6(1-\upsilon^2)}\frac{\partial^2 u}{\partial x^2}+\frac{1}{6(1-\upsilon)}\frac{\partial^2 v}{\partial x\partial y}+\frac{\Delta}{(1+\upsilon)}\frac{\partial^2 u}{\partial y^2}\right)\end{aligned}\tag{43}$$

where $\Delta=(1/4-\alpha(1+\upsilon))$ It is obvious by assigning any values to the unattributed stiffness parameters the residuals of fourth and third order terms in the mid and boundary nodes will not vanish and neither their sums. Residuals in Eq. (43), apart from some constants, are

$$\begin{bmatrix}\frac{1}{12}-\Delta & \frac{1}{12}-\frac{\Delta}{2} & \frac{\Delta}{2}\\ \frac{1}{6}-\Delta & \frac{1}{6}-\frac{\Delta}{2} & \frac{\Delta}{2}\end{bmatrix}\begin{Bmatrix}\frac{\partial^2 u}{\partial x^2}\\ \frac{\partial^2 v}{\partial x\partial y}\\ \frac{\partial^2 u}{\partial y^2}\end{Bmatrix}\tag{44a}$$

To address these two conflicting requirements, one may minimize the columns sums of the coefficient matrix:

$$\begin{bmatrix}\frac{1}{8}-\Delta & \frac{1}{8}-\frac{\Delta}{2} & \frac{\Delta}{2}\end{bmatrix}\begin{Bmatrix}\frac{\partial^2 u}{\partial x^2}\\ \frac{\partial^2 v}{\partial x\partial y}\\ \frac{\partial^2 u}{\partial y^2}\end{Bmatrix}\tag{44b}$$

Column sums of the coefficient matrix in Eq. (44b) are minimized to reduce the cumulative (bias) error in estimates of equation of motion coefficients in each node. The difference between the obtained cumulative (bias) errors and the discretization errors in Eq. (44a) are

$$\begin{bmatrix}-1/24 & -1/24 & 0\\ 1/24 & 1/24 & 0\end{bmatrix}\begin{Bmatrix}\frac{\partial^2 u}{\partial x^2}\\ \frac{\partial^2 v}{\partial x\partial y}\\ \frac{\partial^2 u}{\partial y^2}\end{Bmatrix}\tag{44c}$$

The above expression clearly indicates even distribution of discretization errors with opposite signs in internal and boundary nodes.

Minimizing these cumulative errors in least squares sense leads to

$$\alpha=\frac{1}{8(1+\upsilon)}\tag{45}$$

Substituting Eq. (45) into Eq. (42), the term with q^{-1} represents the boundary conditions. Next the parameter β is obtained by minimizing the error in the boundary requirements formed using the terms in Eqs. (41) and (42) with coefficient q. The same procedure as in Eq. (44a) is followed to determine the remaining parameter β by considering terms with coefficient q in Eqs. (41) and (42). The result is

$$\beta=\frac{7}{24(1-\upsilon^2)}\tag{46}$$

The obtained stiffness matrix provides the highest possible accuracy at internal, boundary and corner nodes and compared with linear displacement assumption (LDA) and linear stress assumption (LSA) formulations has much faster convergence rates.

To obtain unknown parameters of mass matrix, the fourth order terms on the mid nodes and the third order terms on the plane edges are considered, respectively:

$$\begin{aligned}&\frac{1}{q(1-\upsilon^2)}\frac{\partial^2}{\partial x^2}\left(\frac{1}{12}\frac{\partial^2 u}{\partial x^2}+\frac{1+\upsilon}{12}\frac{\partial^2 v}{\partial x\partial y}+\frac{1-\upsilon}{8}\frac{\partial^2 u}{\partial y^2}-\gamma\frac{\partial^2 u}{\partial t^2}\right)\\&\frac{1}{q(1-\upsilon^2)}\frac{\partial}{\partial x}\left(\frac{1}{6}\frac{\partial^2 u}{\partial x^2}+\frac{1+\upsilon}{6}\frac{\partial^2 v}{\partial x\partial y}+\frac{1-\upsilon}{8}\frac{\partial^2 u}{\partial y^2}-\gamma\frac{\partial^2 u}{\partial t^2}\right)\end{aligned}\tag{47}$$

where $\gamma=(2m_{15}+2m_{14}+1/3+m_{12}-m_{16}-2m_{11})$ Assigning any values to the unknown mass parameters the residuals will not vanish and neither their sums. Residuals in Eq. (47), apart from some constants, are

$$\begin{bmatrix}\frac{1}{12}-\gamma & \frac{1}{12}-\frac{\gamma}{2} & \frac{1}{8}-\frac{\gamma}{2}\\ \frac{1}{6}-\gamma & \frac{1}{6}-\frac{\gamma}{2} & \frac{1}{8}-\frac{\gamma}{2}\end{bmatrix}\begin{Bmatrix}\frac{\partial^2 u}{\partial x^2}\\ \frac{\partial^2 v}{\partial x\partial y}\\ \frac{\partial^2 u}{\partial y^2}\end{Bmatrix}\tag{48}$$

Minimizing these cumulative errors in least squares sense leads to

$$\left(2m_{15}+2m_{14}+\tfrac{1}{3}+m_{12}-m_{16}-2m_{11}\right)=\tfrac{23}{144}\tag{49}$$

In least square sense, the second equation of (40) which contains coefficient of q, represents the governing equations if one restricts the entries of mass matrix as,

$$\tfrac{1}{6}-2m_{14}-m_{12}=\tfrac{13}{72}\tag{50}$$

In order to minimize discretization errors, m_{16} and m_{12} are determined from Eqs. (40) to (41) as

$$m_{16}=0;\quad m_{12}=\frac{-1}{72}\tag{51}$$

Applying all these requirements reduces the number of unattributed mass parameters to one. The remaining mass parameter m_{11} is obtained by minimizing the errors of sixth order terms on the mid nodes and five order terms on the boundary nodes. The sixth-order terms at the internal nodes and the five-order terms at the boundary nodes are, respectively:

$$\frac{1}{(1-\upsilon^2)}\frac{\partial^4}{\partial x^2\partial y^2}\left(\frac{25}{1440}\frac{\partial^2 u}{\partial x^2}+\frac{20(1+\upsilon)}{1440}\frac{\partial^2 v}{\partial x\partial y}+\frac{15(1-\upsilon)}{1440}\frac{\partial^2 u}{\partial y^2}-\psi\frac{\partial^2 u}{\partial t^2}\right) \tag{52}$$

$$\frac{1}{(1-\upsilon^2)}\frac{\partial^3}{\partial x\partial y^2}\left(\frac{50}{1440}\frac{\partial^2 u}{\partial x^2}+\frac{30(1+\upsilon)}{1440}\frac{\partial^2 v}{\partial x\partial y}+\frac{15(1-\upsilon)}{1440}\frac{\partial^2 u}{\partial y^2}-\psi\frac{\partial^2 u}{\partial t^2}\right) \tag{53}$$

where $\psi=(m_{11}-138/1728)$ Minimizing the bias errors, m_{11} is determined as,

$$m_{11}=\tfrac{23}{216} \tag{54}$$

The proposed mass matrix provides the highest possible accuracy at the internal and boundary nodes whilst producing the same order of error as the bi-linear shape functions (BDR) element on the corner nodes. In what follows the improvement of the new model in predicting the plane stress behavior is demonstrated.

5. Numerical examples

Three test cases are used to demonstrate the efficiency of the new plane stress element. Static and dynamic behavior of a plane stress element is predicted using the proposed formulation and compared with those obtained from established shape-function formulations.

The first case study is a cantilever beam with aspect ratio of 1/30 where its mesh and loading conditions are shown in Fig. 6 similar to Felippa's [10] and MacNeal and Harder [19]. The beam has module of elasticity of 1e7 Pa, Poisson's ratio of 0.3, length of 1 m, and thickness of 1 mm. A unit (1 N) concentrated shear force is applied to the beam end with the exact tip deflection of $\delta=(PL^3/3EI_z)+(PL/GA)=0.1080780$, where G is shear module and I_z is the cross section moment of inertia. The results of tip deflection modeled with six elements are shown in Table 1. The proposed model in this paper is compared with linear stress assumption (LSA) [3], constant strain triangle (CST) [20], strain mode [21], and linear displacement assumption (LDA) [2] element formulations. The LDA and CST elements suffer from in-plane bending problem as the other three formulations predict the tip deflection with improved accuracy and the proposed model produces the best results.

The second example evaluates the behavior of a thick cantilever beam of unit length with aspect ratio of $h/L=1/3$ as shown

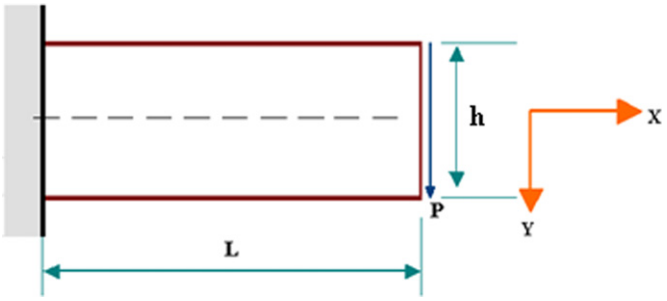

Fig. 6. Geometry, boundary conditions and loading of the cantilever beam.

Table 1
Estimated beam tip deflection (the exact solution 0.1080780).

Element type	Tip deflection
Constant strain triangle (CST) [20]	0.005044
Linear displacement assumption (LDA) [2]	0.010088
Linear stress assumption (LSA)[3]	0.10023
Strain mode element, MSC/NASTRAN [21]	0.096
Proposed model	0.10225

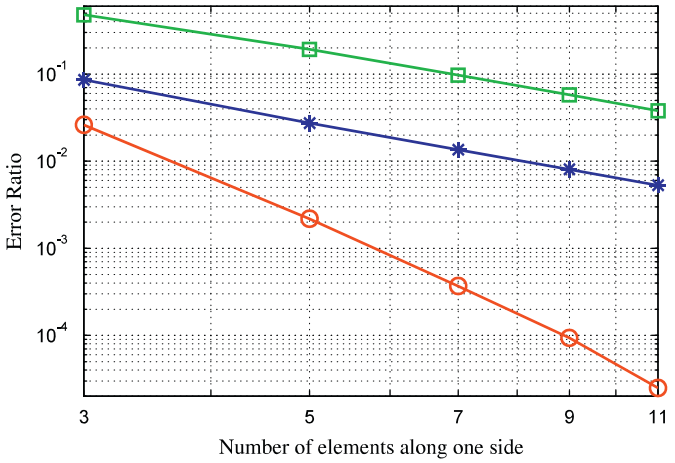

Fig. 7. Errors in estimating the tip deflection ($q=1/3$, $v=0.3$) (circle – proposed model, star – LSA, and square – LDA).

in Fig. 6. Increasing the number of elements along the X-axis, Felippa [10] showed that the assumed stress element has better accuracy than Allman triangle with drilling freedoms [22], CST [20], and strain mode element [21]. Many researchers have used the same problem as a test case for the in-plan bending elements. From the existing models, the results of LSA [3] formulation and LDA [2] formulation are listed; the parameters of the LSA and LDA formulations are the closest to the optimum values hence, produce smaller errors compared to other models reported in the literature. The value of shear force is unity (1 N), module of elasticity 1000 Pa, thickness is 1 mm, the Poisson ratio is 0.3 and the exact solution of displacement is 116.33 mm. Fig. 7 shows the non-dimensional error of tip deflection plotted as a function of number of elements along one side of the model. Comparing the values obtained using the LSA, LDA and the new formulations; one notices a significant improvement in predicting the static behavior of the beam using the new formulation. Next the beam height is reduced to $h=L/6$. The loading remains the same but the exact tip deflection increases to 873.33 mm. Fig. 8 shows the error of non-dimensional tip deflection plotted as a function of number of elements. It can be seen that the new proposed model is more accurate and has fast convergence in predicting the exact solution compared to LSA and LDA model predictions.

In the third case study in-plane vibrations of a square plate with various boundary conditions are considered [23]. The rate of convergence in the fundamental frequency of in-plane motion is determined with proposed mass and stiffness matrices and compared with LDA and LSA models predictions. In the study convergence of fundamental eigen-value of a square plate in dimensionless form is considered. The dimensionless form of eigen-value is $\lambda^2=\omega a\sqrt{\rho(1-v^2)/E}$. The plate with side length a is isotropic with modulus E, the Poisson ratio v, volumetric mass density ρ, and circular frequency of vibration ω. The results for two different cases of free and clamped boundary conditions are

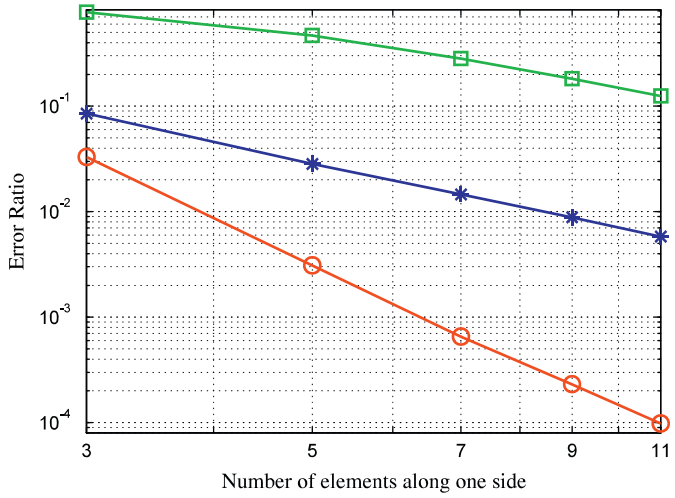

Fig. 8. Errors in estimating the tip deflection ($q=1/6$, $\nu=0.3$) (circle – proposed model, star – LSA, and square – LDA).

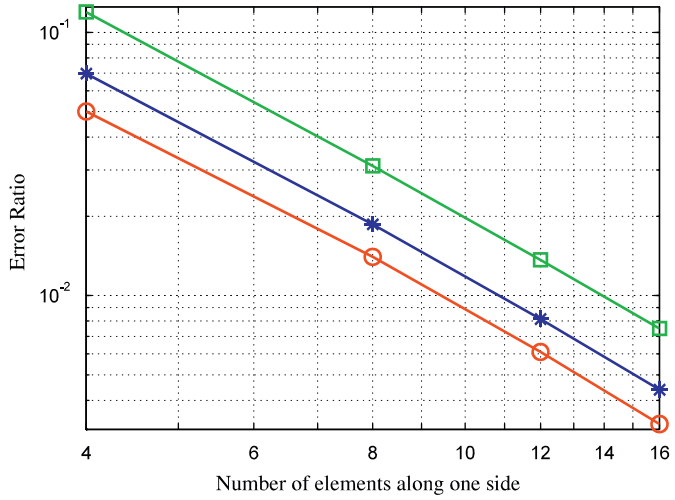

Fig. 9. Rate of convergence in estimating the fundamental frequency of a free square plate in in-plane motion (circle – proposed model, star – LSA, and square – LDA).

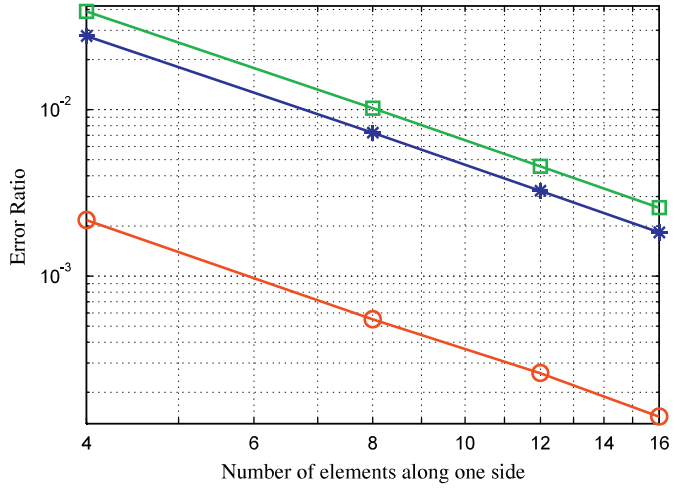

Fig. 10. Rate of convergence in estimating the fundamental frequency of a clamped square plate in in-plane motion (circle – proposed model, star – LSA, and square – LDA).

shown in Figs. 9 and 10, respectively. As it can be seen from these figures the proposed model produces superior results compared to other those models.

6. Conclusion

New stiffness and mass matrices for plane stress and transverse membrane elements are presented using an inverse approach. In the inverse approach, the criteria that element model must satisfy is considered and a parametric family of admissible stiffness and mass matrices are formed. The parameters of the element model are then obtained by minimizing the discretization errors in the element formulation. In minimizing the discretization errors, special attention is paid on reducing the sum of errors over the assembled model nodes hence creating a model with minimum bias errors. New formulation developed for rectangle plane stress element improves static and eigenvalues problems considerably in comparison with the best model presented in previous studies. The improvements in elements formulation are demonstrated using numerical case studies. The added accuracy in the new models requires no extra computational effort and it may be implemented easily into the existing finite element codes.

References

[1] I. Fried, M. Chavez, Superaccurate finite element eigenvalue computation, J. Sound Vib. 275 (2004) 415–422.
[2] J.H. Argyris, S. Kelsey, Energy Theorems and Structural Analysis, Butterworths, London, 1960 (Part I reprinted from Aircr. Eng. 26 October 1954).
[3] J.S. Przemieniecki, L. Berke, Digital computer program for the analysis of aerospace structures by the matrix displacement method, Flight Dyn. Lab Rep. FDL (1964) 18–64.
[4] P.G. Bergan, C.A. Felippa, A triangular membrane element with rotational degrees of freedom, Comput. Methods Appl. Mech. Eng. 50 (1985) 25–69.
[5] T.T.H. Pian, Derivation of element stiffness matrices by assumed stress distributions, J. AIAA 2 (1964) 1333–1336.
[6] E.L. Wilson, R.L. Taylor, W. Doherty, J. Ghaboussi, Incompatible displacement models, Num. Comput. Methods Struct. Mech. (1973) 43–57.
[7] R.L. Taylor, P.J. Beresford, E.L. Wilson, A nonconforming element for stress analysis, Int. J. Numer. Methods Eng. 10 (1976) 1211–1219.
[8] M. Froier, L. Nilsson, The rectangular plane stress element by Turner Pain and Wilson, Int. J. Numer. Methods Eng. 8 (1974) 433–437.
[9] R.H. Gallagher, Finite Element Analysis Fundamentals, Prentice-Hall, Englewood Cliffs, NJ, 1975.
[10] C.A. Felippa, Supernatural Quad 4: a template formulation, Comput. Methods Appl. Mech. Eng. 195 (2006) 5316–5342.
[11] L. Yunhua, A. Eriksson, Extension of field consistence approach into developing plane stress elements, Comput. Methods Appl. Mech. Eng. 173 (1999) 111–134.
[12] J.H. Argyris, M. Haase, H.P. Mlejnek, On an unconventional, but natural formulation of a stiffness matrix, Comput. Methods Appl. Mech. Eng. 22 (1980) 1–22.
[13] P.G. Bergan, M.K. Nygard, Finite elements with increased freedom in choosing shape function, Int. J. Numer. Methods Eng. 20 (1984) 643–663.
[14] J.C. Simo, M.S. Rifai., A class of mixed assumed strain methods of incompatible modes, Int. J. Numer. Methods Eng. 29 (1990) 1595–1638.
[15] C. Stavrinidis, J. Clinckemaillie, J. Dubois, New concepts for finite element mass matrix formulation, J. AIAA 27 (1989) 1249–1255.
[16] H. Ahmadian, M.I. Friswell, J.E. Mottershead, Minimization of the discretization error in mass and stiffness formulation by an inverse method, Int. J. Numer. Methods Eng. 41 (1998) 371–387.
[17] S. Rao, Vibration of Continues Systems, John Wiley & Sons, 2007.
[18] A.H. Nayfeh, Linear and Nonlinear Structural Mechanics, Jon Wiley & Sons, 2007.
[19] R.H. MacNeal, R.L. Harder, A proposed standard set of problems to set finite element accuracy, Finite Elem. Anal. Des. 1 (1985) 3–20.
[20] M.J. Turner, R.W. Clough, H.C. Martin, L.J. Topp, Stiffness and deflection analysis of complex structures, J. Aerosci. 23 (1956) 805–824.
[21] R.H. MacNeal, The evolution of lower order plate and shell elements in MSC/NASTRAN, in: T.J.R. Hughes, E. Hinton (Eds.), Finite Element Methods for Plate and Shell Structures Element Technology, vol. I, Pineridge Press, Swansea, UK, 1986, pp. 85–127.
[22] D.J. Allman, Evaluation of the constant strain triangle with drilling rotations, Int. J. Numer. Methods Eng. 26 (1988) 2645–2655.
[23] D.J. Gorman, Free in-plane vibration analysis of rectangular plates by the method of superposition, J. Sound Vib. 272 (2004) 831–851.